Cubed-sphere modelling activities at CSIRO

John McGregor

CSIRO Oceans and Atmosphere

Aspendale, Melbourne

Acknowledgement: Marcus Thatcher

NCEP

Washington DC

16 May 2019

Overview

CCAM is a variable-resolution AGCM, developed from 1997 on the conformal-cubic grid

Reversible grid and dynamics finalized 2005

Many physics options added

Coupled ocean recently added (also on C-C grid) and sea-ice

Highly vectorized with MPI, running up to 14,000 cores

CCAMe – equal-area version (uniform Jacobian grid)

CCAMf – flux form of dynamical core (also on equal-area grid)

CCAM is mainly used for specialized NWP and climate downscaling

Alternative cubed-sphere grids

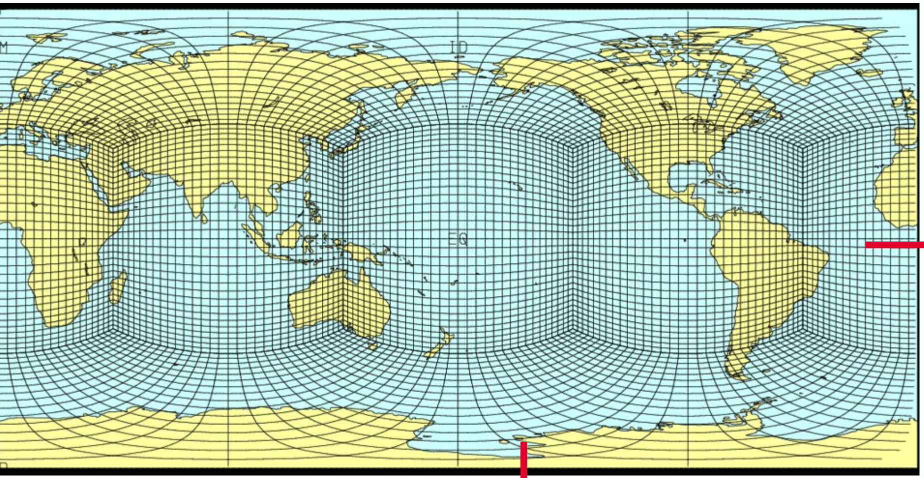

Original Sadourny gnomonic grid

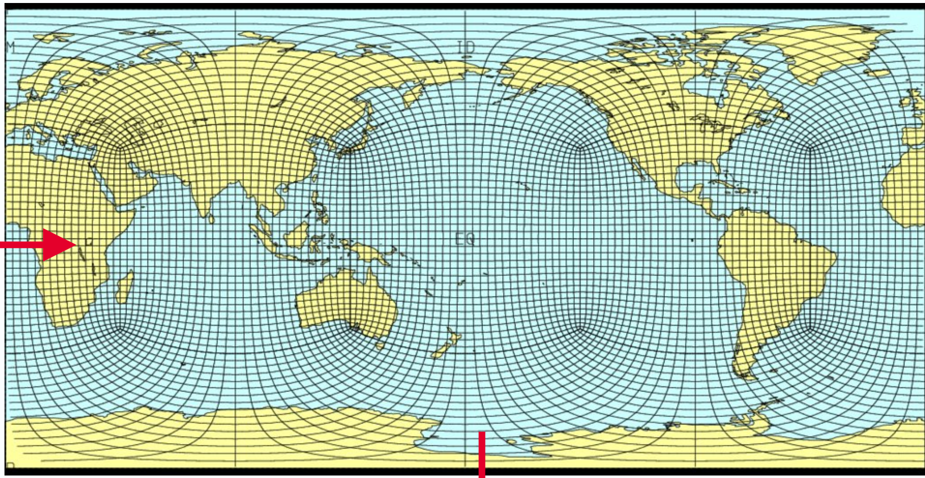

Conformal cubic (Rancic et al.)

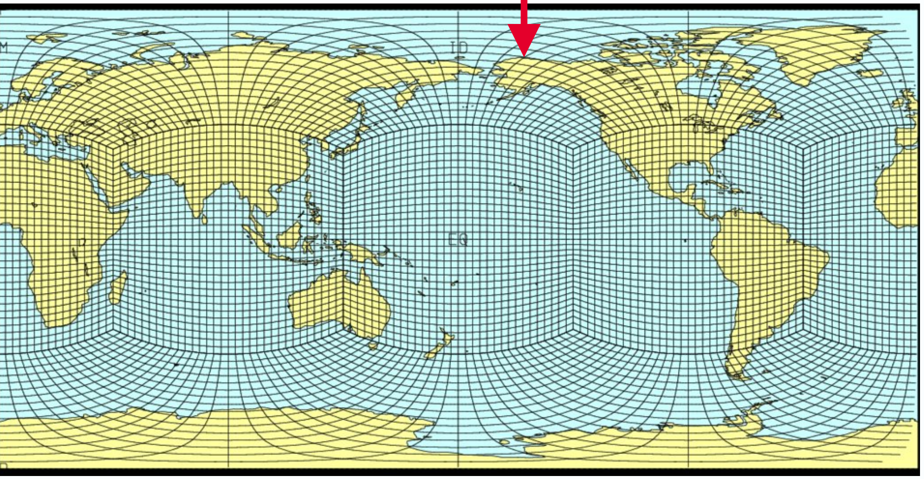

Equi-angular gnomonic grid

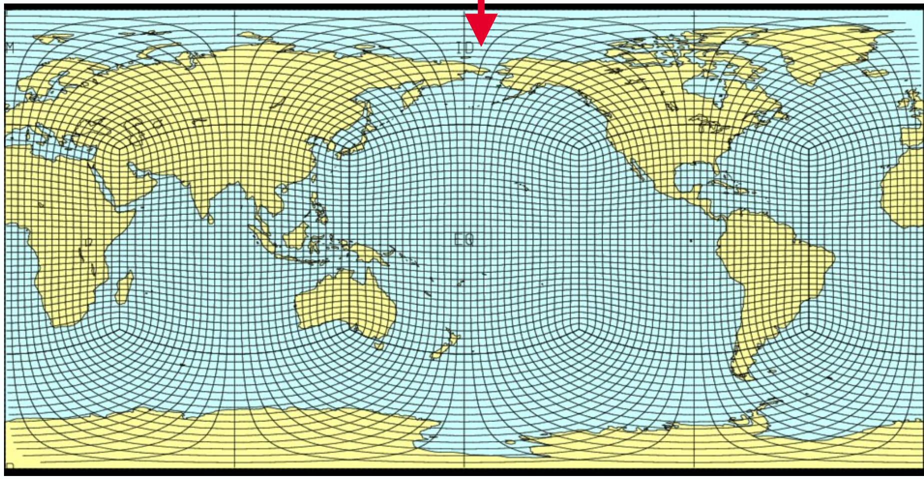

Uniform Jacobian (equal area)
(Purser and Rancic)

All C32

Vertex views of C48 grids

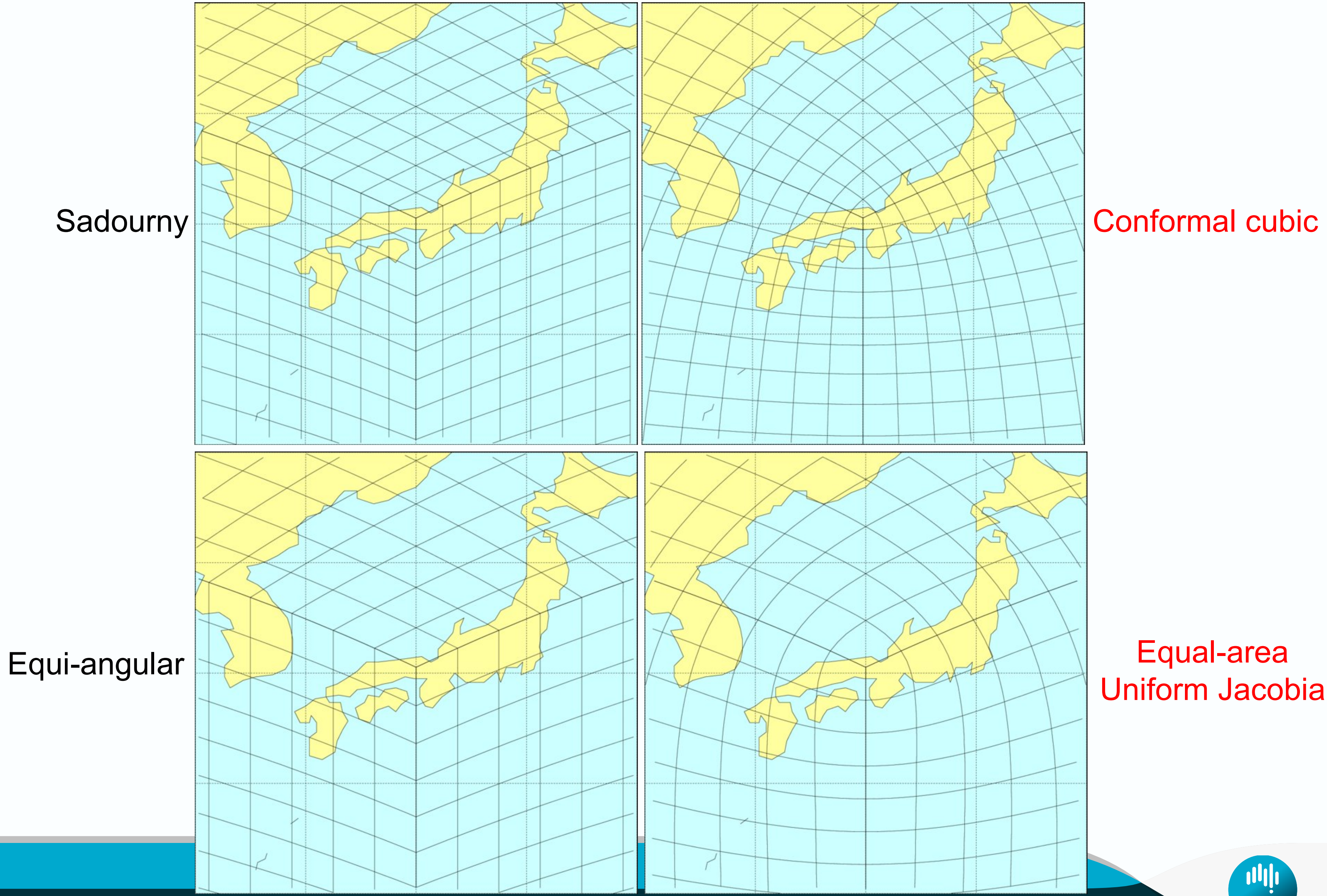

The conformal-cubic atmospheric model

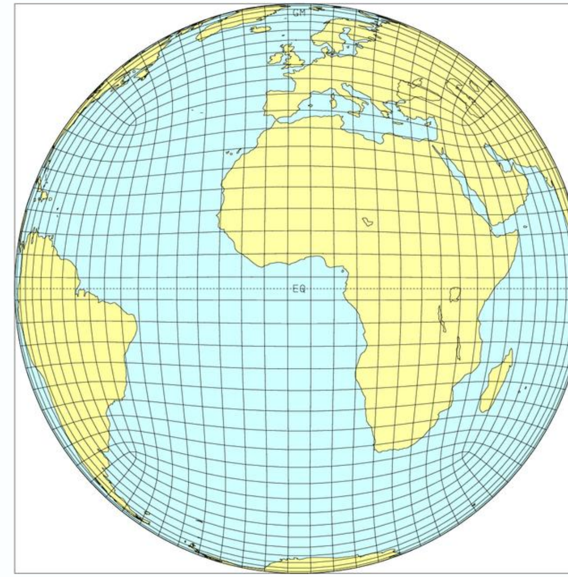

CCAM is formulated on the conformal-cubic grid

Reversible staggering

Miller-White non-hydrostatic (extremely efficient)

Schmidt transformation stretched-grid capability for higher resolution

Semi-Lagrangian

Orthogonal

Isotropic

Parallel I/O

Good scaling

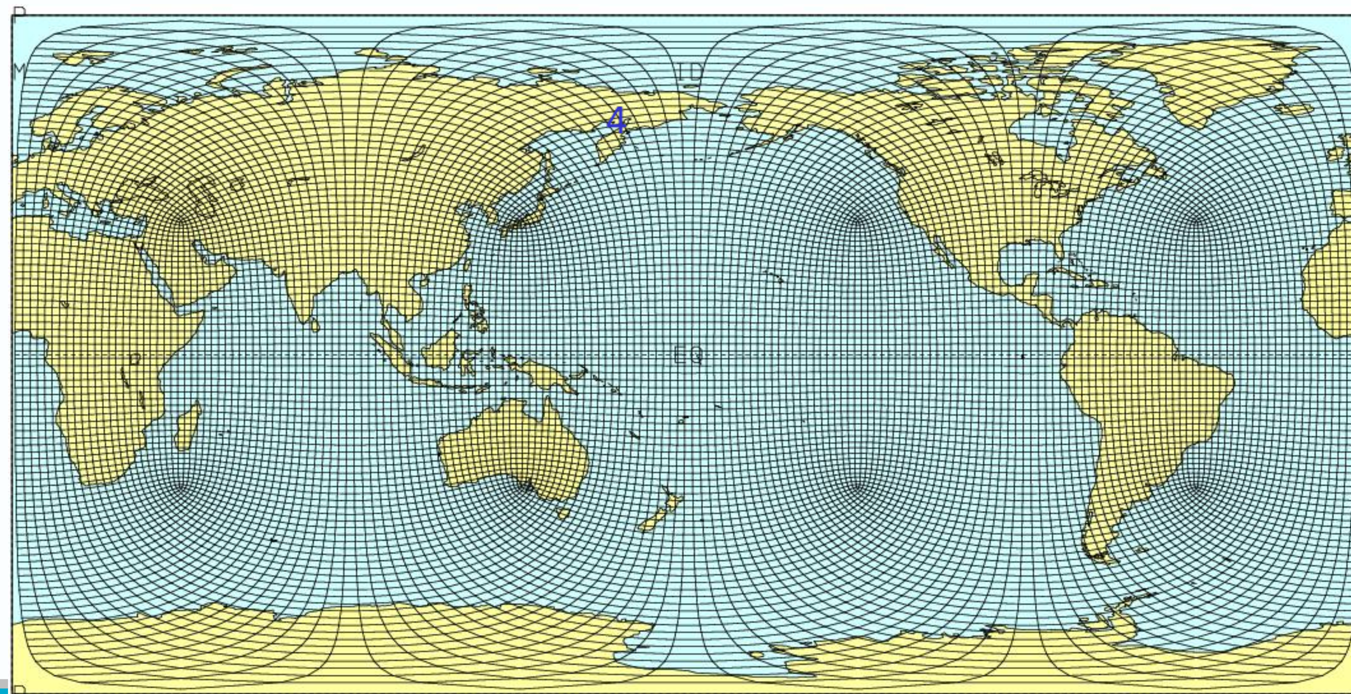

Quasi-uniform C96 grid with resolution about 100 km (showing every 2nd point)

Location of variables in grid cells

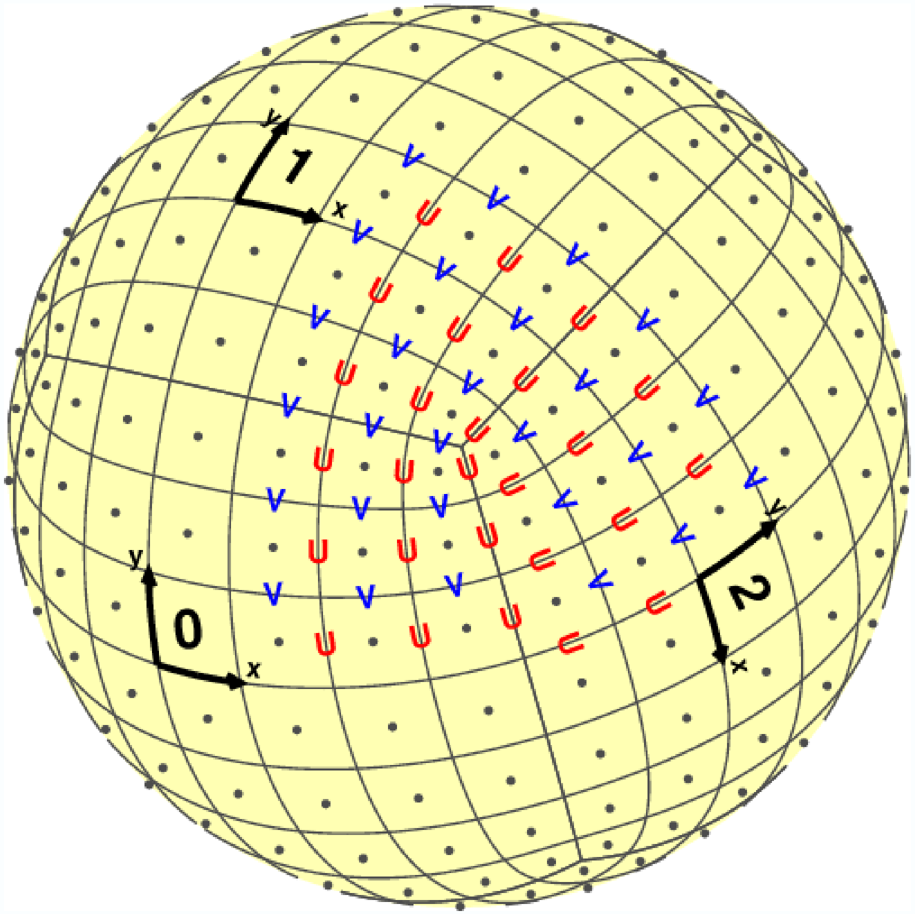

All variables are located at the centres of quadrilateral grid cells.

In CCAM, during semi-implicit/gravity-wave calculations, u and v are transformed reversibly to the indicated C-grid locations.

Produces same excellent dispersion properties as spectral method (see McGregor, MWR, 2006), but avoids any problems of Gibbs' phenomena.

2-grid waves preserved. Gives relatively lively winds, and good wind spectra.

Reversible staggering

pivot

| X | X * | X |

m-1 m-1/2 m m+1/2 m+1 m+3/2 m+2

m+3/4

Where u is the staggered velocity component and U is the Unstaggered value, can write

$$\frac{3u_{m+1/2} + u_{m+3/2}}{4} = \frac{U_m + 3U_{m+1}}{4}$$

or higher order (using Vandermonde formula)

$$\frac{u_{m-1/2} + 10u_{m+1/2} + 5u_{m+3/2}}{16} = \frac{5U_m + 10U_{m+1} + U_{m+2}}{16}$$

Accurate at the pivot points for up to 4th order polynomials

Solved iteratively (u $\rightarrow$ U or U $\rightarrow$ u), or by cyclic tridiagonal solver over 4 faces of the cube

Excellent dispersion properties for gravity waves

- also leads to good kinetic energy spectra

Dispersion behaviour for linearized shallow-water equations

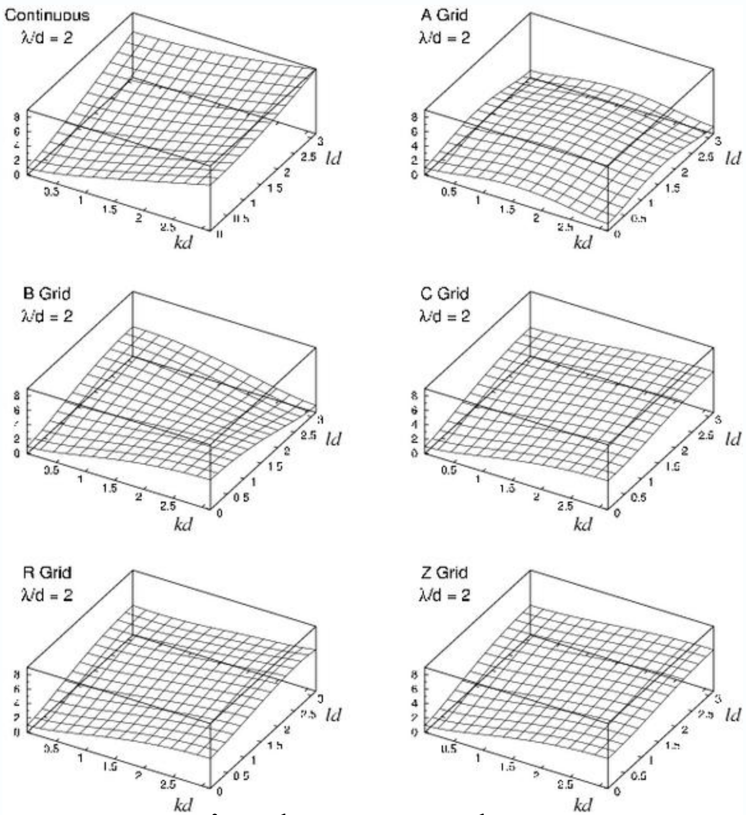

Typical atmosphere case

- large radius of deformation

-R grid, Z grid and spectral models all extremely similar

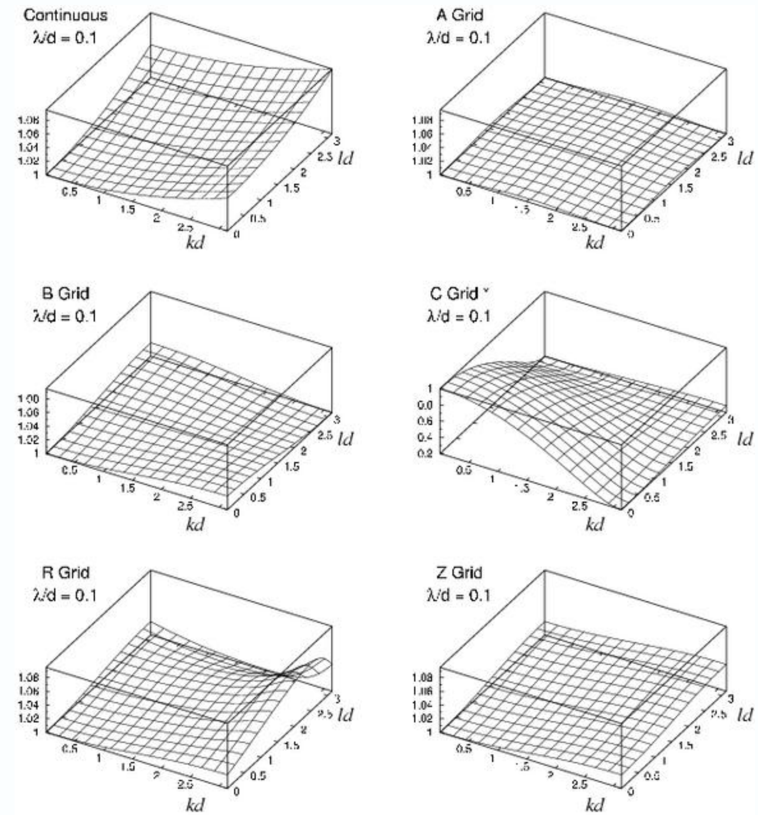

Typical ocean case

- small radius of deformation

N.B. the (ocean) asymmetry of the R grid response disappears by alternating the reversing direction each time step, giving the same response as Z (vorticity/divergence) grid

Kinetic energy spectra

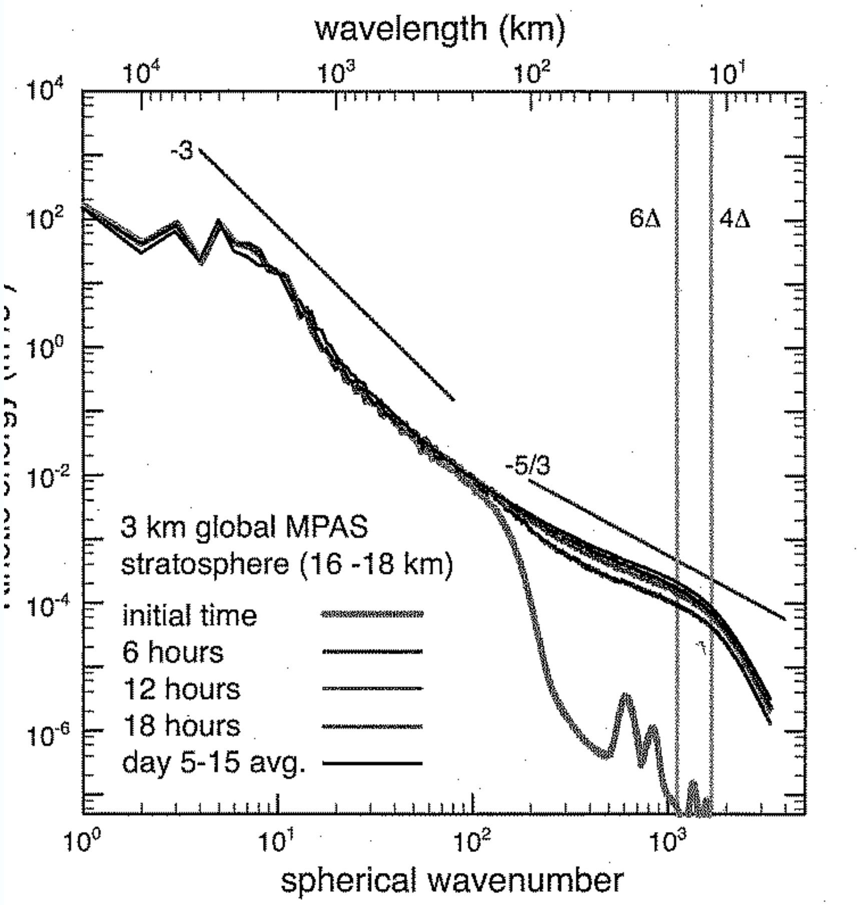

3 km MPAS
Skamarock et al. (2014)

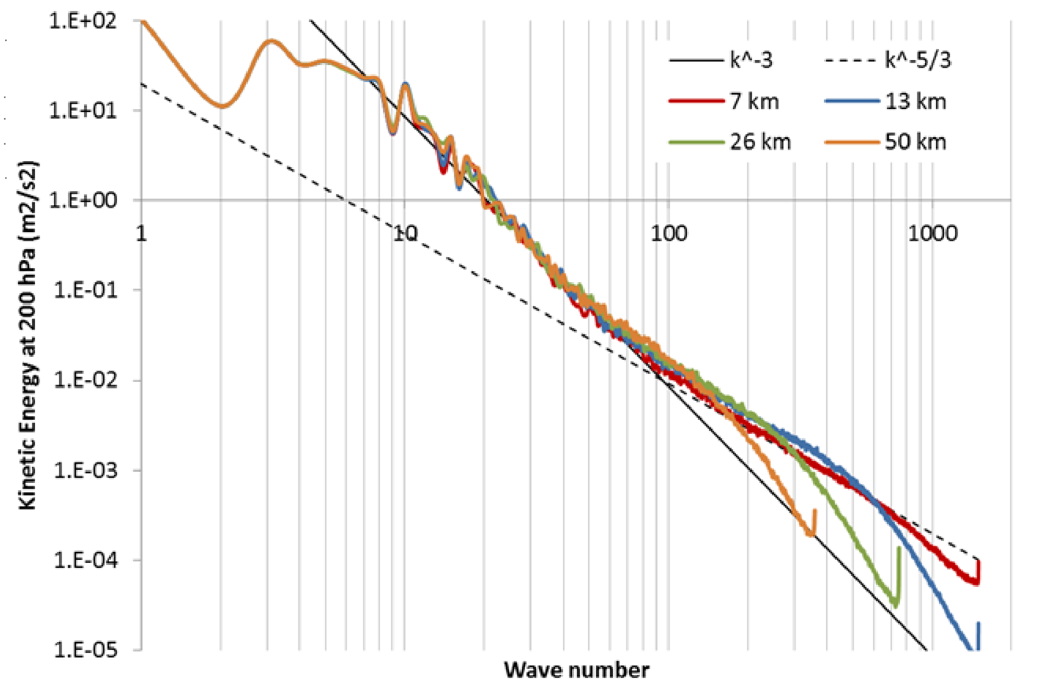

CCAM 7 km to 50 km grids
(RH curving up is just an artefact of the diagnostic routine)

CCAMe – equal-area dynamical core

- similar numerics to CCAM, but formulated on the (non-orthogonal) equal-area Uniform Jacobian grid
- employs covariant and contravariant wind components, used for advection, etc.
- provides uniform resolution
- semi-Lagrangian, semi-implicit time-stepping
- reversible staggering transforms the winds to the staggered positions needed for calculating divergence and gravity-wave terms
- requires a larger stencil for the Helmholtz equation (whilst also using vertical eigenvector decomposition)
  - readily solved using multigrid
- uses CCAM special treatments near orography and for nonhydrostatic treatment

a posteriori conservation

- *a posteriori* conservation of mass and moisture for semi-Lagrangian CCAM and CCAMe
- “global” scheme
- simultaneously ensures non-negative values
- during each time step applies correction to changes occurring during dynamics (including advection)
- correction is proportional to the “dynamics” increment, but the sign of the correction depends on the sign of the increment at each grid point.
- This scheme is compared quite favourably with other schemes by Michail Diamantakis (GMD 2013).

The above are described in the CCAM Tech. report 2005

Semi-Lagrangian treatment of p_s advection

Semi-Lagrangian pressure advection in continuity equation

$$\left\{\ln p_s + (1+\varepsilon_a)\frac{\Delta t}{2}\left(D + \frac{\partial \dot\sigma}{\partial \sigma}\right)\right\}^{\tau+1} = \left\{\ln p_s - (1-\varepsilon_a)\frac{\Delta t}{2}\left(D + \frac{\partial \dot\sigma}{\partial \sigma}\right)\right\}^{\tau *}$$

Define an associated variable, similar to MSLP

$$\ln \breve{p}_s = \ln p_s + \frac{z_s g}{R_d \overline{T}_k},$$

which varies smoothly, even over terrain. It is thus suitable for evaluation by bi-cubic interpolation, whilst the added term is found "exactly" by bi-linear interpolation (to avoid any overshooting effects). Formally, get

$$(\ln p_s)^* = (\ln \breve{p}_s)^* - \left(\frac{z_s g}{R_d \overline{T}_k}\right)^*.$$

Semi-Lagrangian nonhydrostatic treatment

The hydrostatic equation for geopotential height ϕ is replaced by the Miller-White equation

$$\underbrace{\frac{R\bar{T}}{g^2}\frac{R}{\sigma}\frac{D}{Dt}\left(T\frac{\omega}{\sigma p_s}\right)}_{\text{Miller-White term}} + \underbrace{\frac{\partial\phi}{\partial\sigma} + \frac{R}{\sigma}T_v = 0}_{\text{Hydrostatic equation}}$$

Prior to updating the u, v equations in the $\Delta t'$ loops, ϕ is normally calculated

$\frac{D}{Dt}\left(T\frac{\omega}{\sigma p_s}\right)$ may be calculated at this time and a modified ϕ calculated.

Being a semi-Lagrangian model, CCAM is able to absorb the extra phi terms into its Helmholtz equation solver, for zero cost

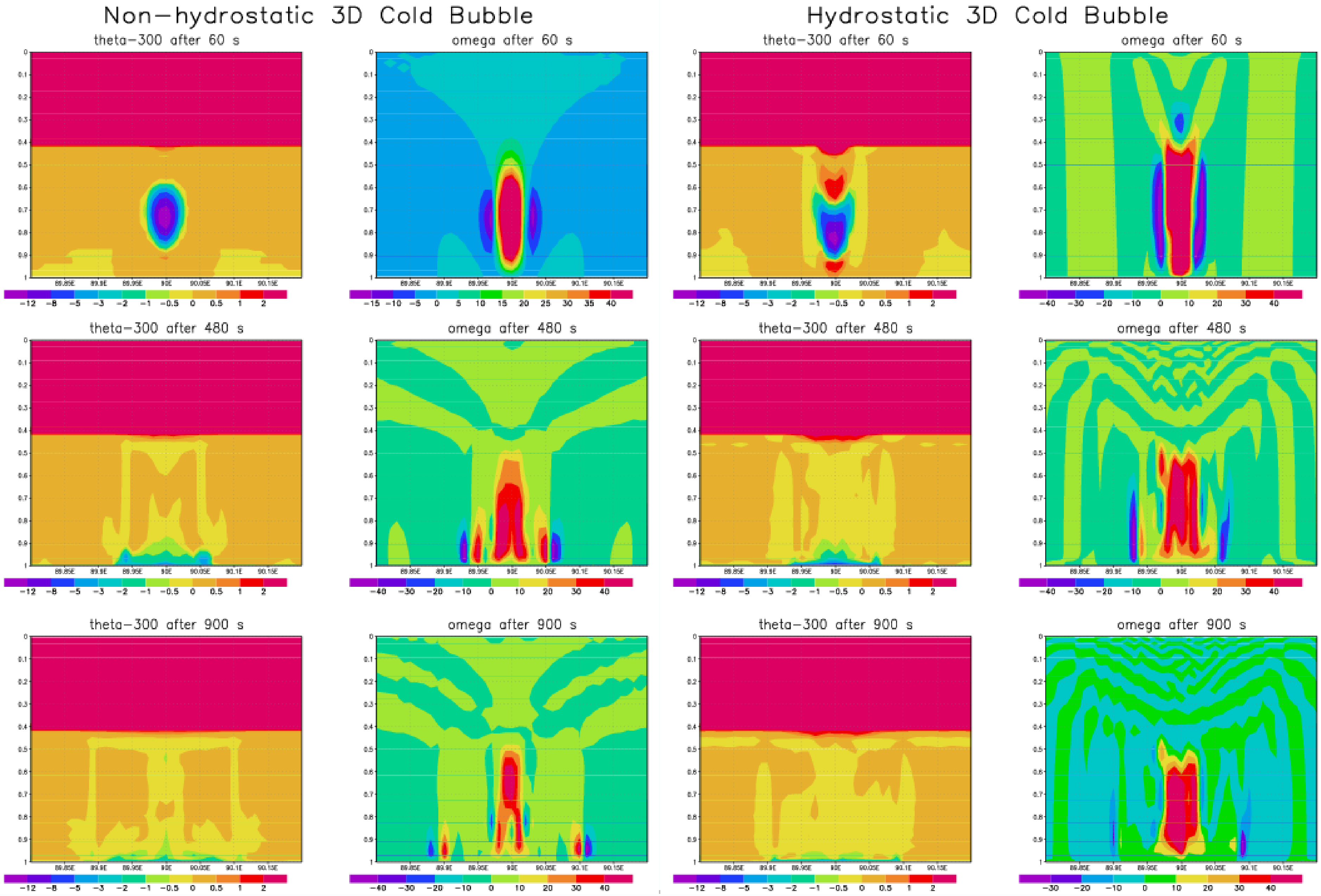

CCAM simulations of cold bubble, 500 m L35 resolution, on highly stretched global grid

Flow over 250 m ridge on a reduced sphere

To compare with 2D test of Schar et al. (2002)

Grid spacing=625 m, L35 and L52, dt=20 s

(MPAS, Klemp et al. (2015) 720 m, dt – 15 s)

radius=rearth/166.7 (6371km to 38.22 km)

Height of ridge = 250 m at equator.

Initially solid body flow with uzon=20 m/s at equator, and isothermal T=300

Showing vertical velocities after 2 h

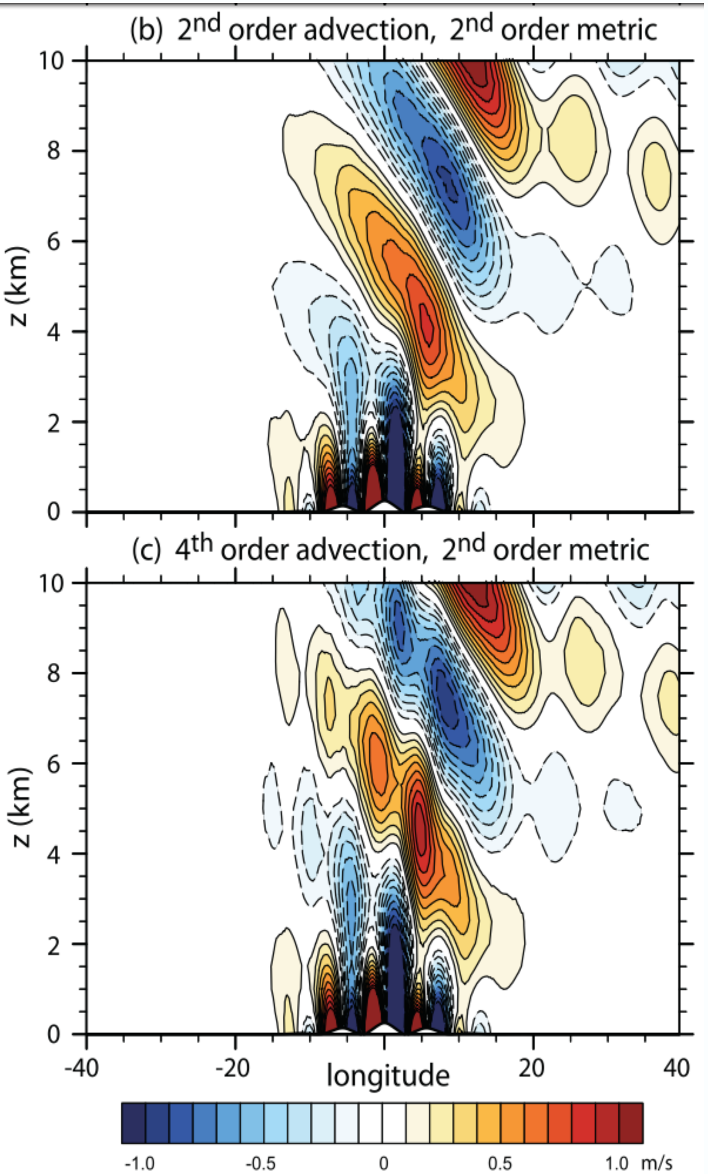

L52

L35

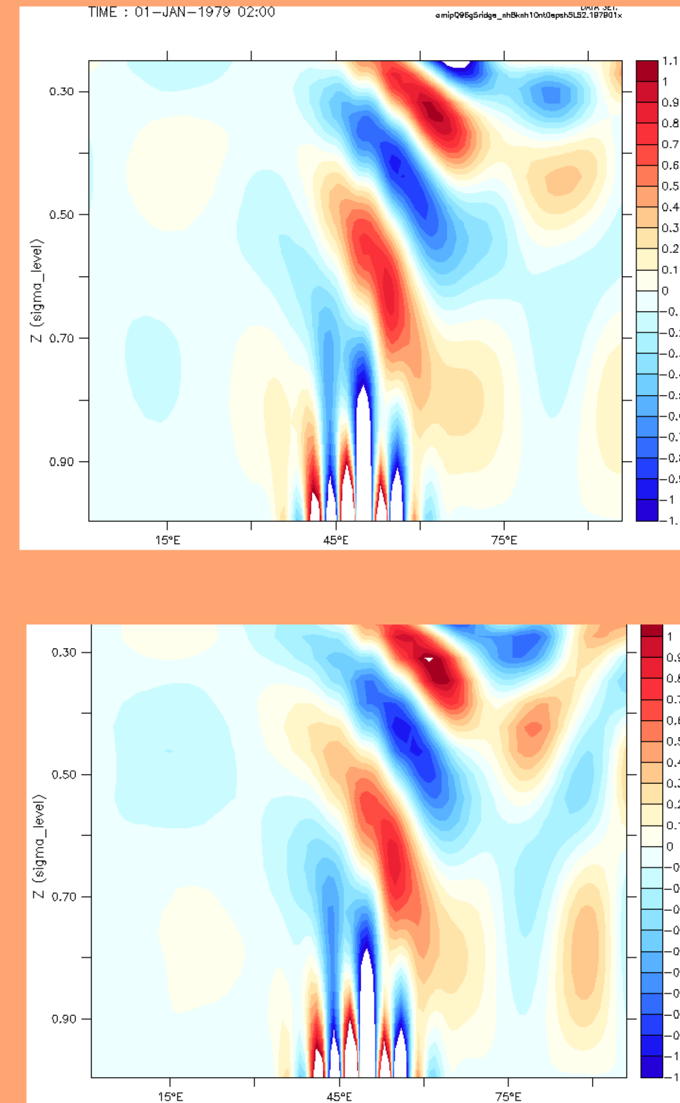

MPAS (Klemp et al.)

CCAM

Behaviour at vertices

vertex

t=1

t=6

2 min

t=12

4 min

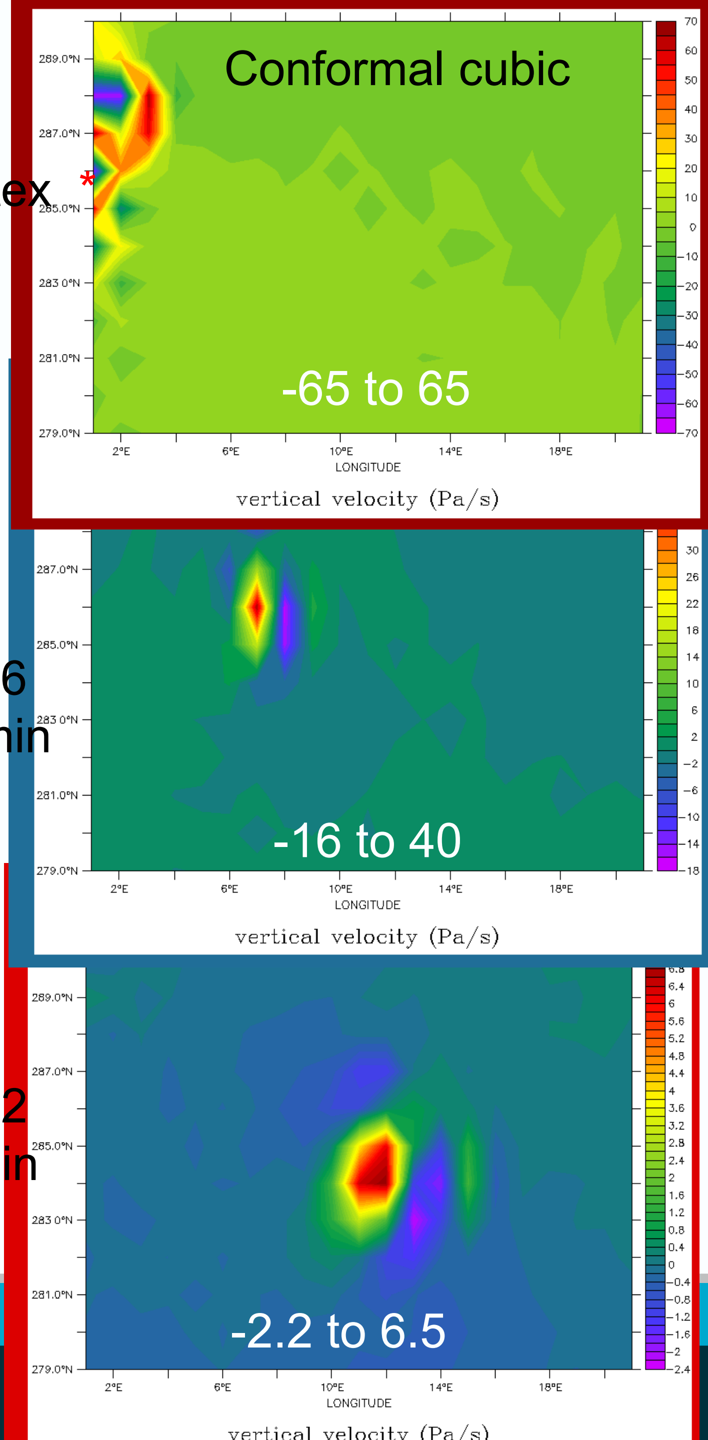

For solid body initial flow, there should be zero initial omega.

At timestep 1 see some spurious omega near vertices.

Only apparent for small grid lengths, e.g. 200 m. Here 625 m

Related to reversible staggering and very strong curvature of grid lines at the vertices.

Flow rapidly adjusts to give zero omega, but the disturbance propagates, decreasing as it propagates

Could treat as an “initialization issue”

vertex *
t=1

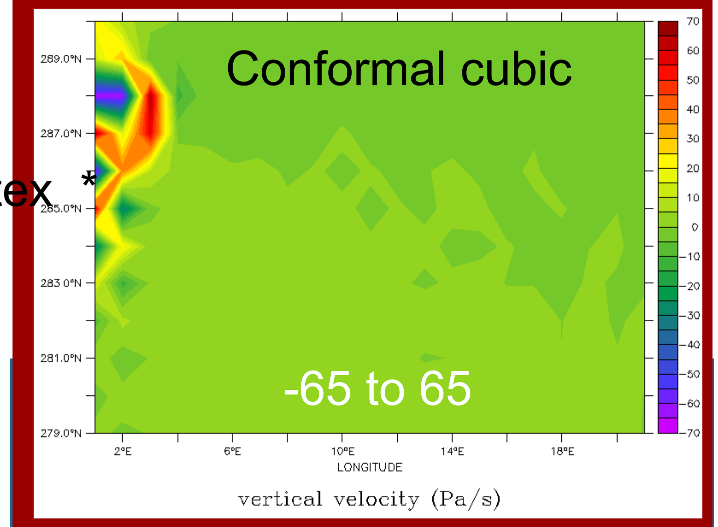

t=6
2min

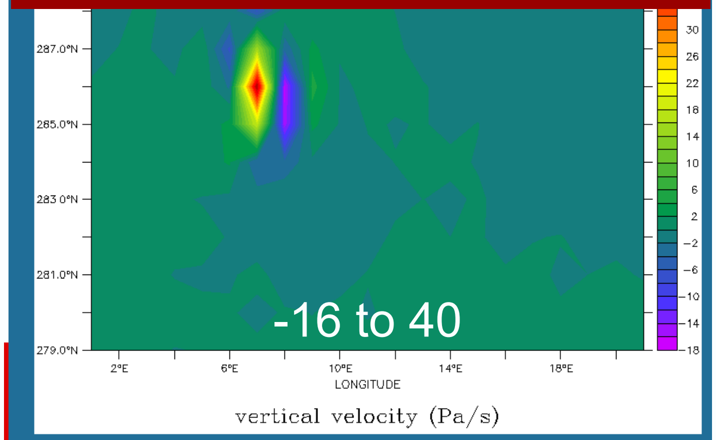

t=12
4min

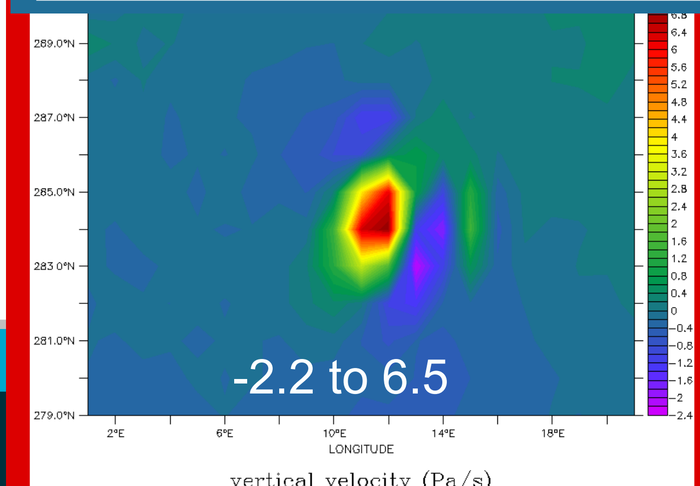

HOWEVER

The problem effectively disappears when using the Uniform Jacobian grid (magnitudes 100 times smaller)

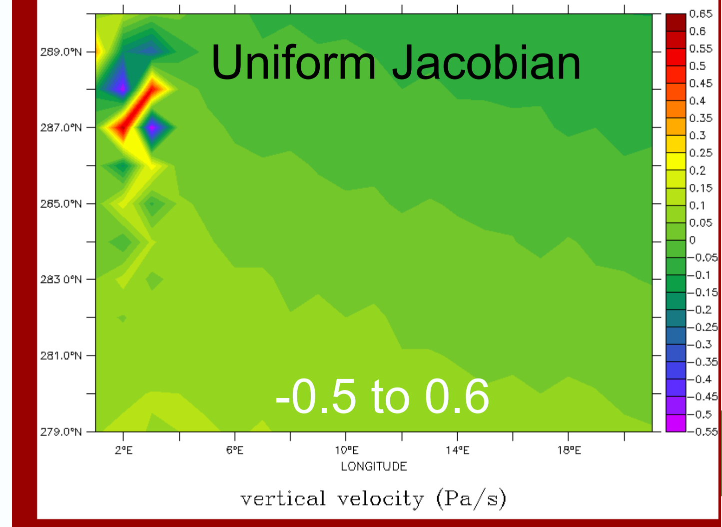

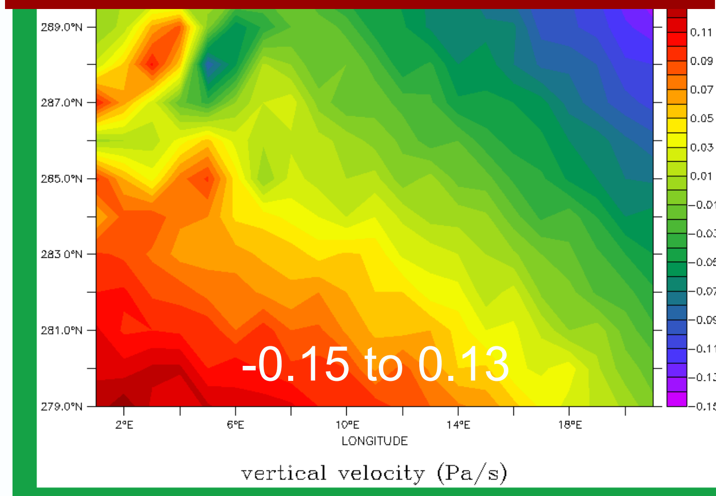

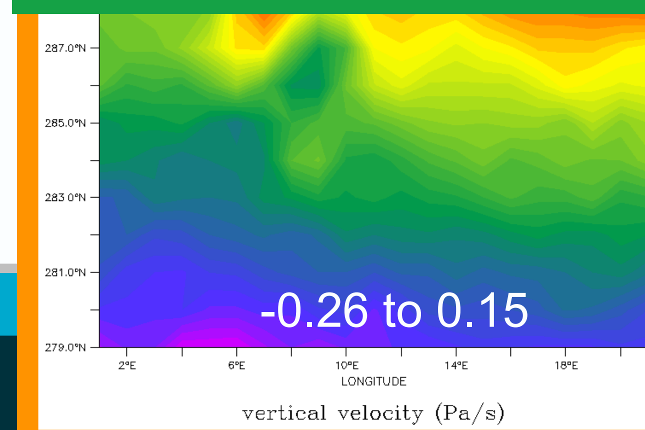

CCAMe status

Same computational efficiency as CCAM

Includes all of the CCAM dynamics features, and the Miller-White non-hydrostatic treatment

Model development is complete, just finalizing aspects of the Schmidt transformation for stretched grid usage, and finalizing changes to the input and output routines.

Provides the atmospheric component of the CSIR/CSIRO coupled model collaboration for CMIP6

Advection in CCAM versions

Advect 3D Cartesian wind components – avoids any issues when crossing panel boundaries, where local (x,y) directions may rotate (also for CCAMe and CCAMf)

Special surface pressure advection (needed for semi-Lagrangian treatment of continuity equation); also CCAMe

Related special T advection to reduce spurious advection effects near orography; also CCAMe

CCAMf - flux conserving dynamical core

- formulated on equal-area (uniform Jacobian) grid
  - also has uniform resolution
- less issues for resolution-dependent parameterizations
- reversible staggering transforms the contravariant (and covariant) winds to the staggered positions needed for calculating divergence and gravity-wave terms
- forward-backward (F-B) split-explicit solver for gravity waves
  - no need for Helmholtz solver
  - linearizing assumptions avoided in gravity-wave terms
  - avoids semi-Lagrangian off-centring issues at mountains
- flux-conserving form of equations
- finite volume advection with TVD preserves sharp gradients
  - Some benefits for trace gas studies
- dynamics has a number of similar features to FV3, though both developed independently

TVD advection

Low-order and high-order fluxes combined using Superbee limiter

Cartesian components (U,V,W) of horizontal wind are advected

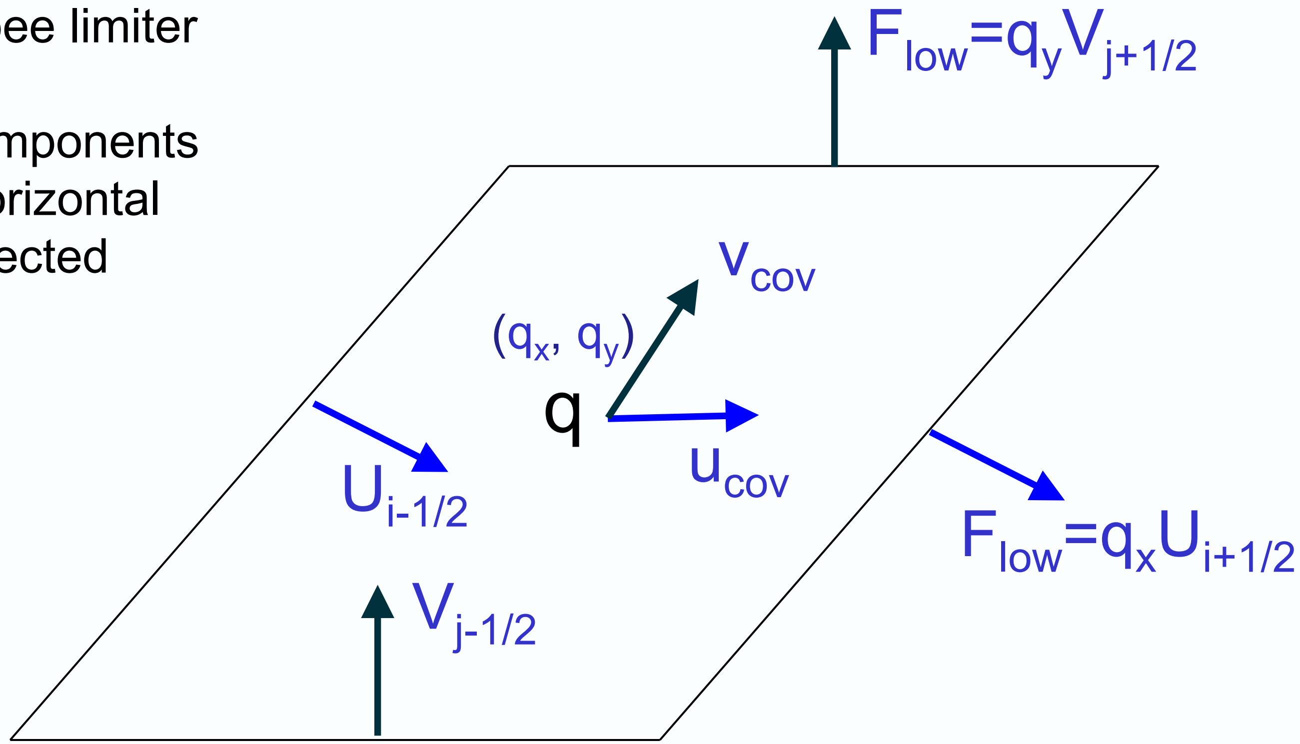

3D transverse components are included in both low and high order fluxes, calculated at the edges of the grid cells. Some similarities to LeVeque method. No grid imprinting is seen, especially when using equal-area grid.

Advection example on equal-area grid

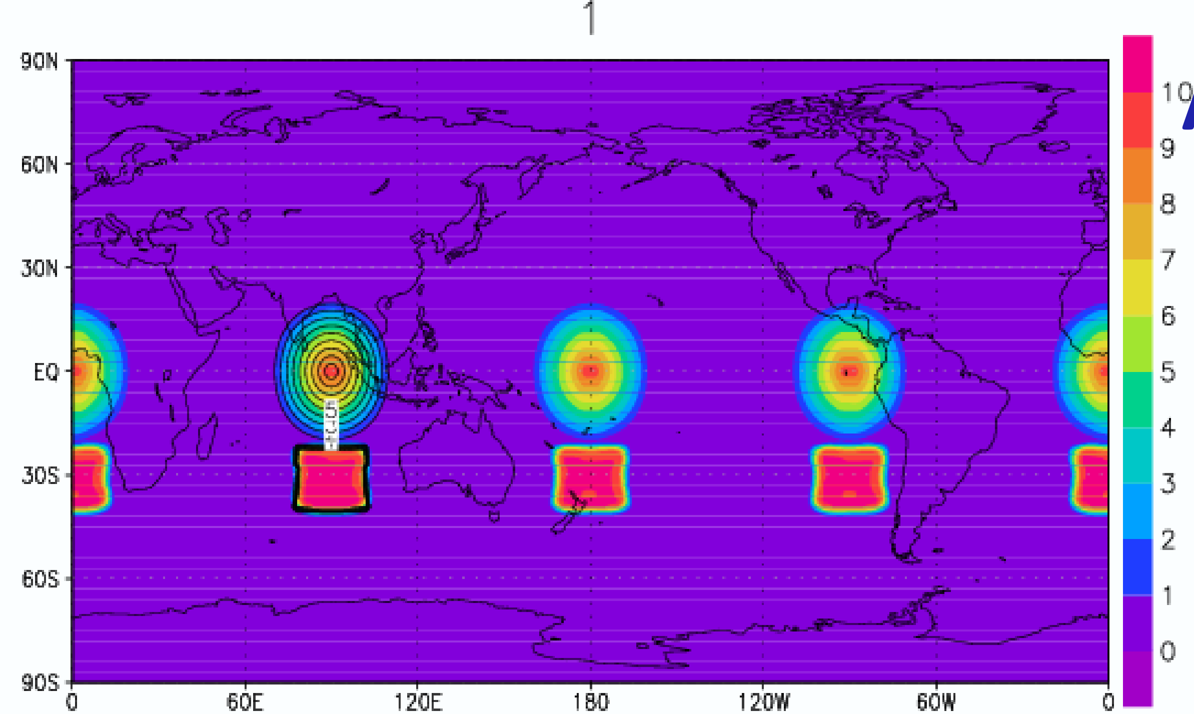

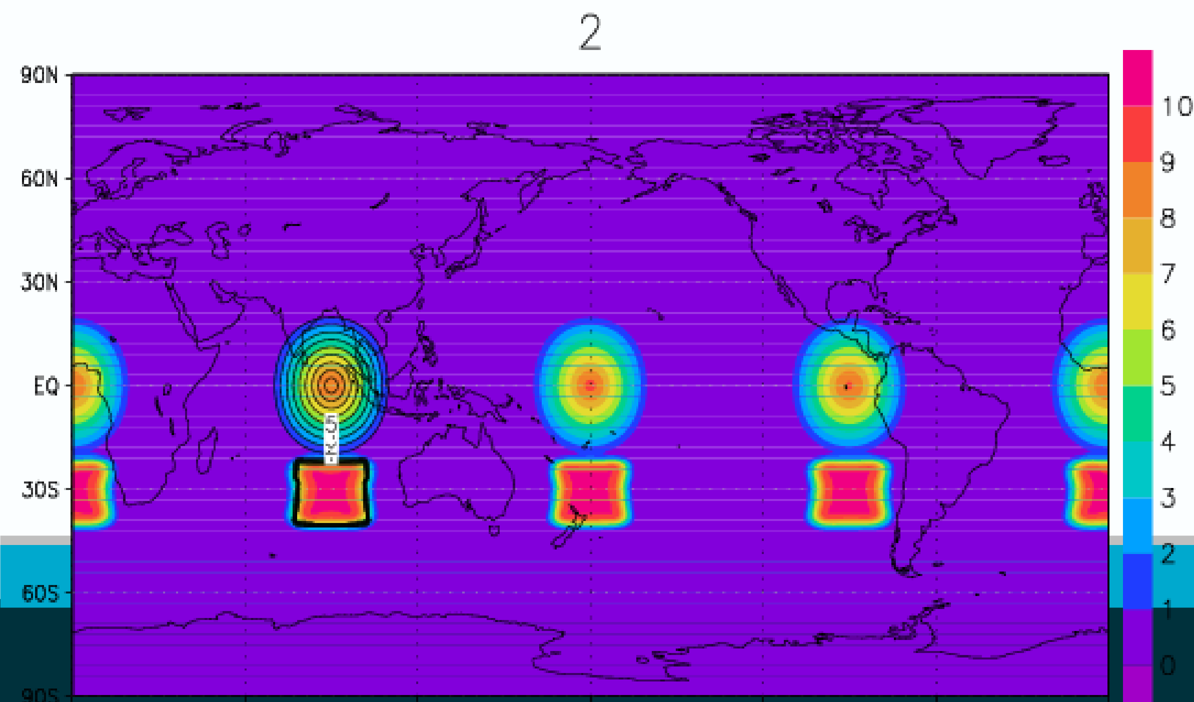

TVD scheme used in CCAMf

Eastwards solid body rotation in 8 days, advecting cone and prism (dt= 15 or 20 mins)

Semi-Lagrangian used in CCAMe

Some alternative options for CCAMf

a) Calculate pressure gradient using first principles. This involves vertical interpolation on adjacent columns. Not expensive because no MPI involved

b) Standard Norm Phillip's differencing on sigma surfaces

c) Hybrid vertical coordinates

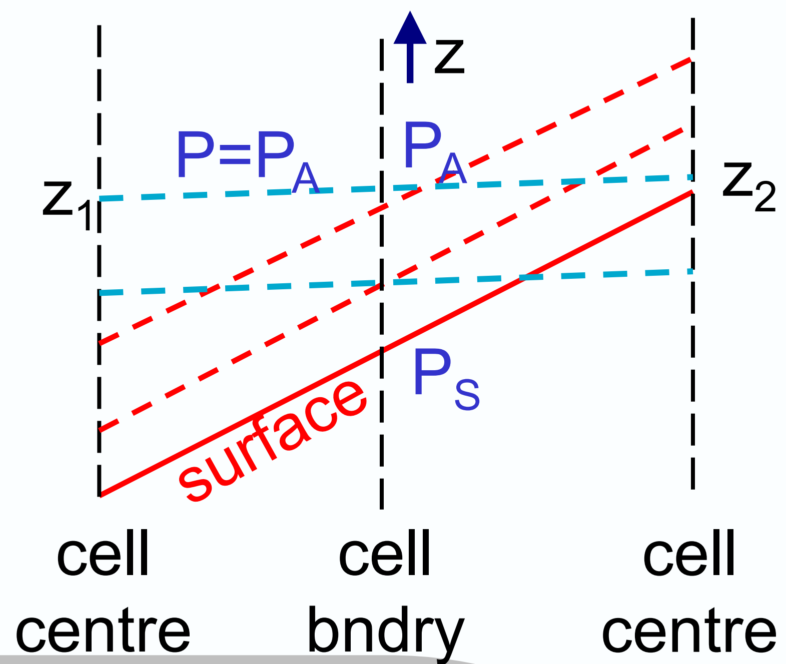

CCAMf status

Originally coding was on equi-angular grid, but hard to avoid small edge effects and grid imprinting

Now settled on the equal-area (Uniform Jacobian) grid

Presently needs small divergence damping at upper levels

Presently bit slower than CCAM

Still need to include non-hydrostatic treatment

– probably HEVI approach

Comparison of CCAMf and CCAMe

CCAMf advantages

No Helmholtz equation needed

Includes full dhi_dx terms in momentum equations

- no T linearization needed

Mass and moisture conserving

No semi-Lagrangian resonance issues near steep mountains (though these seem very rare in CCAM)

Simpler MPI (semi-L "computation on demand" not needed), so scales better for massively parallel computers

CCAMf disadvantages

Restricted to Courant number of 1, but not big problem since grid is very uniform

Nonhydrostatic treatment will be more expensive than Miller-White in CCAM – probably will use HEVI

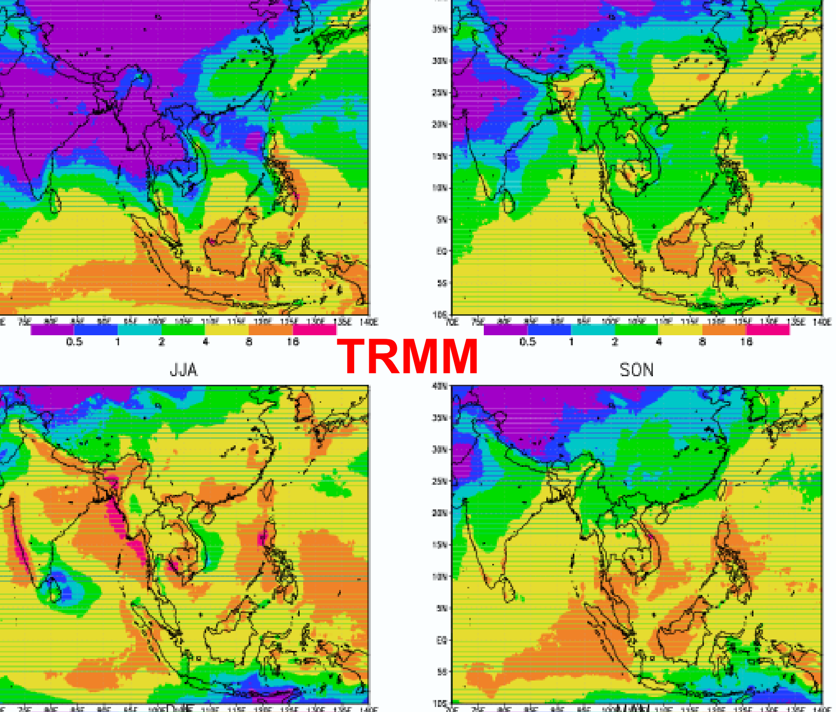

5-year C96 (100 km) runs - precip

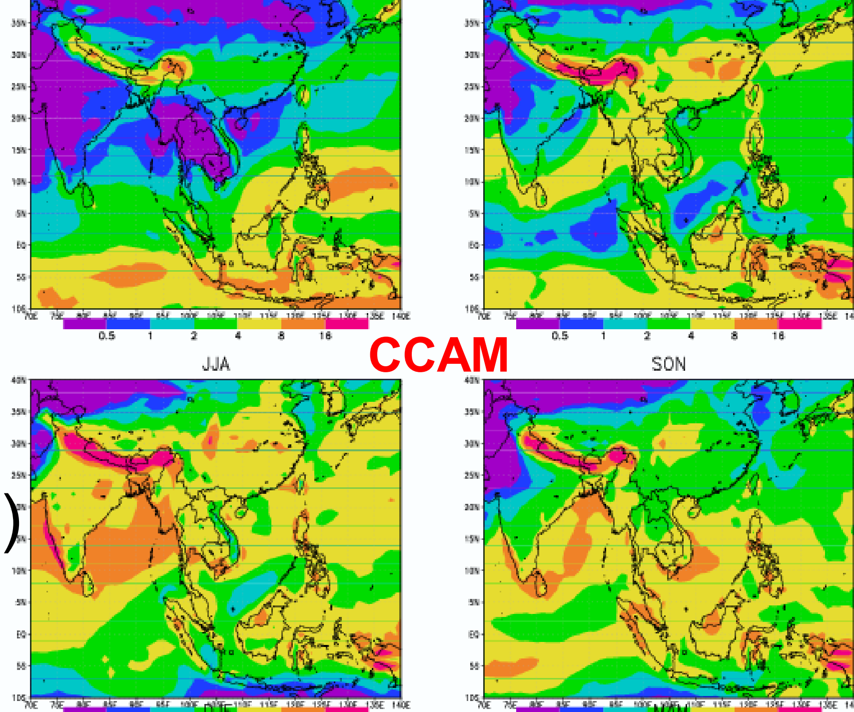

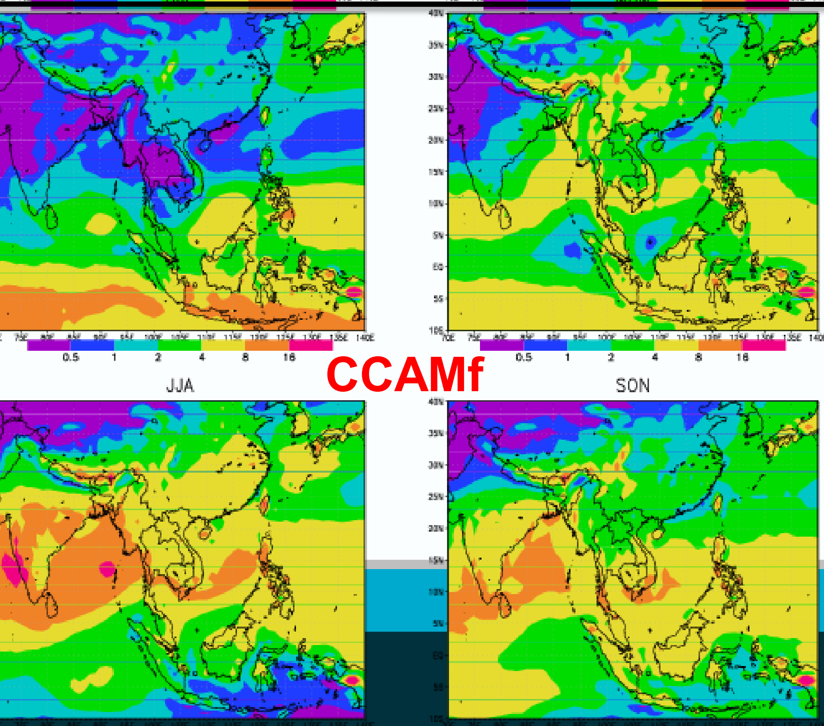

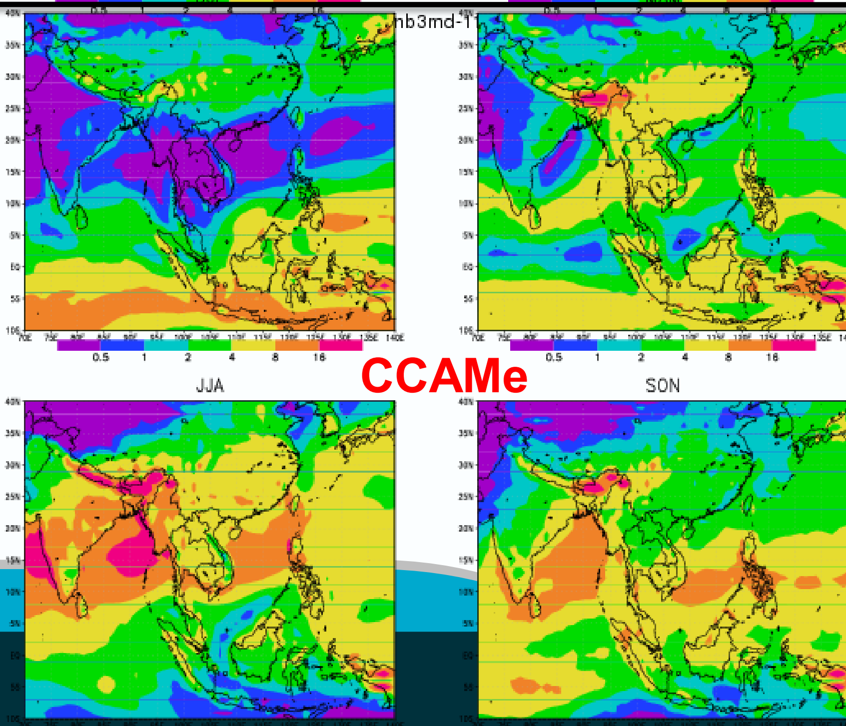

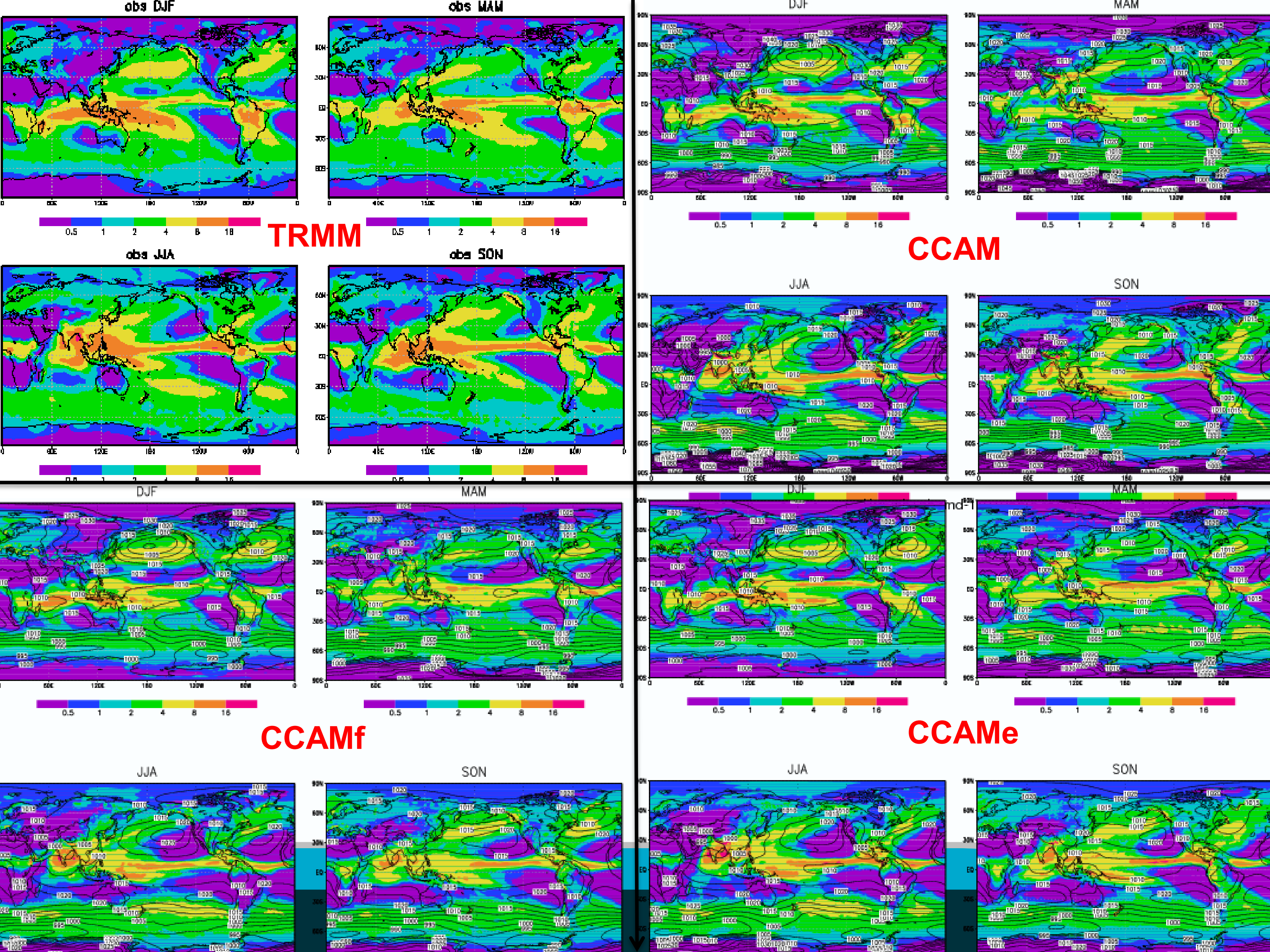
obs DJF
obs MAM
obs JJA
obs SON
0.5 1 2 4 8 16
TRMM
DJF
MAM
JJA
SON
CCAM
CCAMf
CCAMe

Example of wave behaviour

(5y L27 run at 100 km)

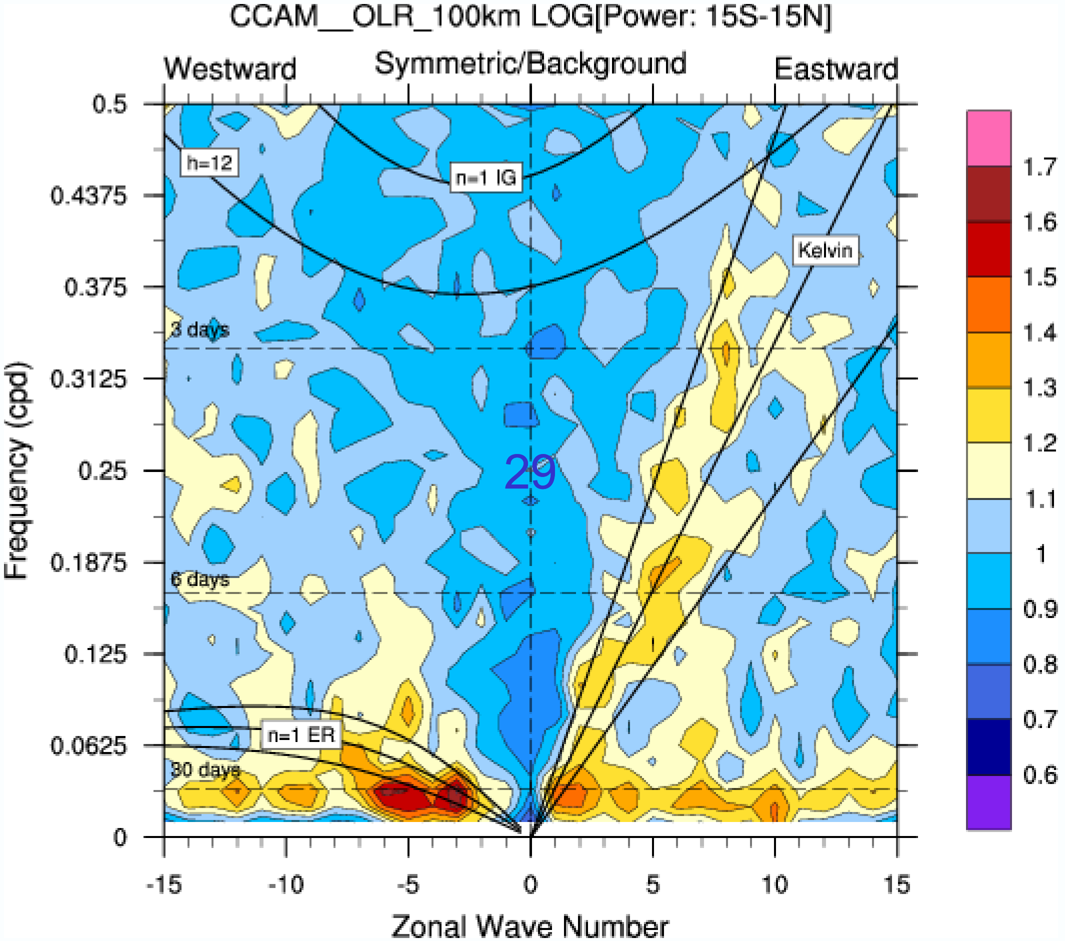

Variable-resolution conformal-cubic grid

The conformal-cubic grid is moved to locate panel 1 over the region of interest.
The Schmidt (1975) transformation is applied

- it preserves the orthogonality and isotropy of the grid
- same primitive equations, but with modified values of map factor

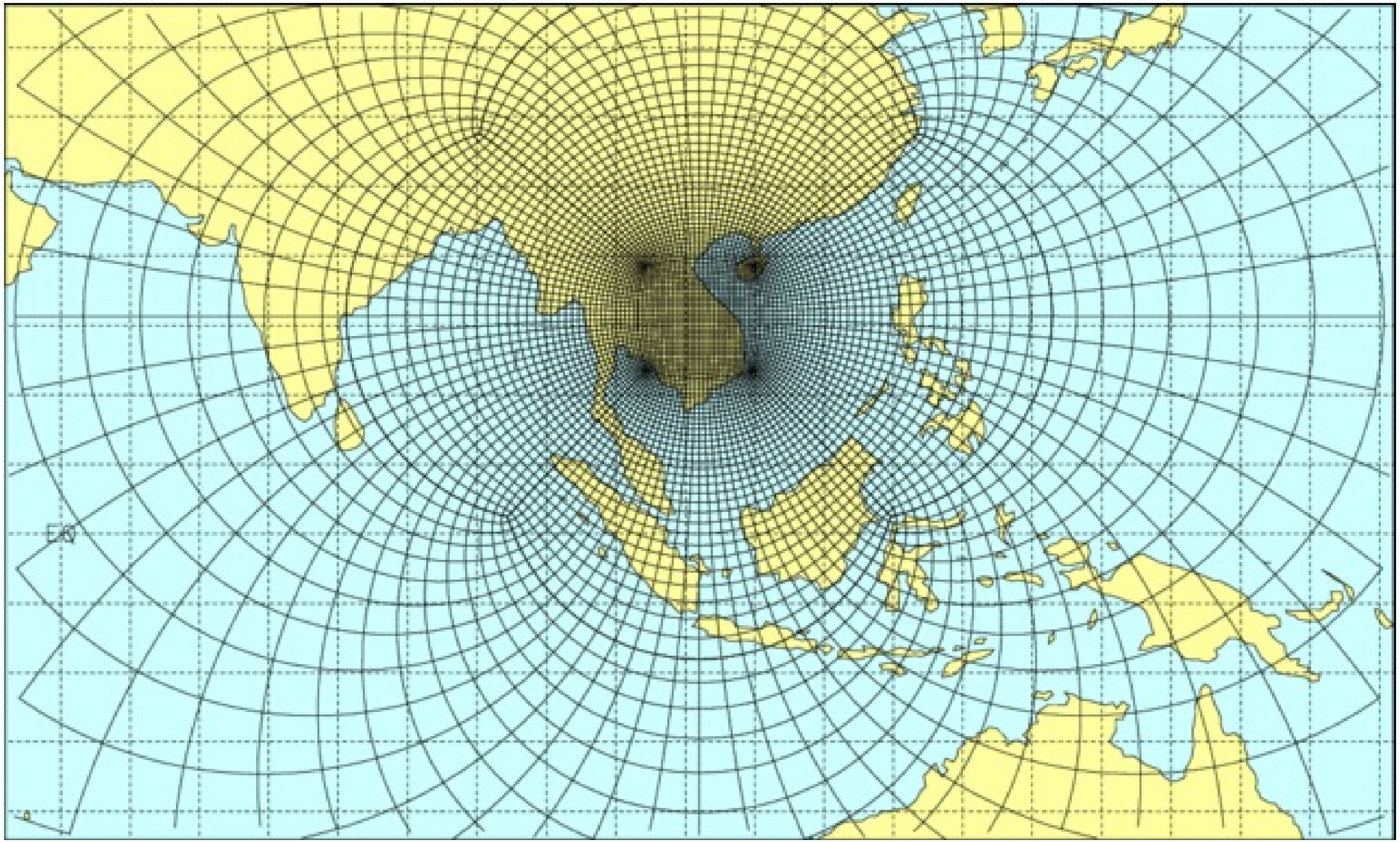

C48 grid (with resolution about 20 km over Vietnam)

CCAM downscaling methodology

First run a quasi-uniform 100 km global CCAM run driven by bias-corrected (for present-day) SSTs

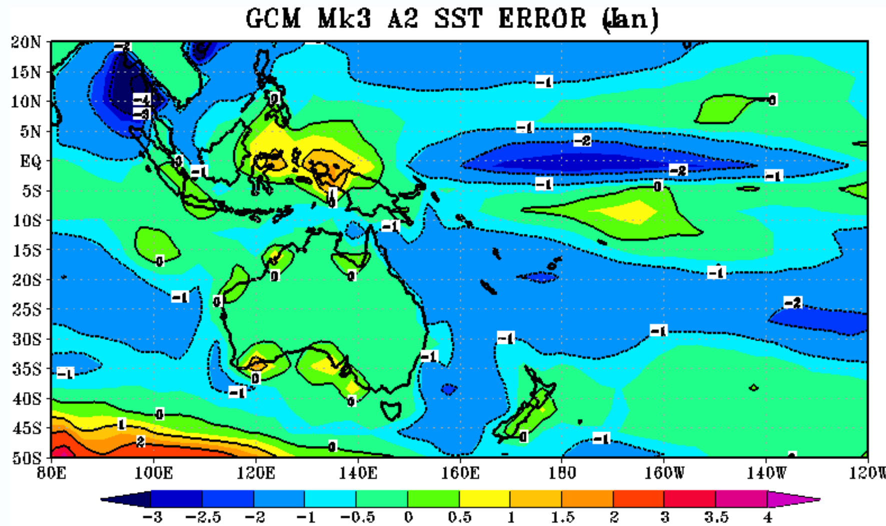

The 100 km run is then downscaled to 20 km (or finer) by running CCAM with a stretched grid, but applying a digital filter every 3 to 6 h to preserve large-scale patterns of the 100 km run

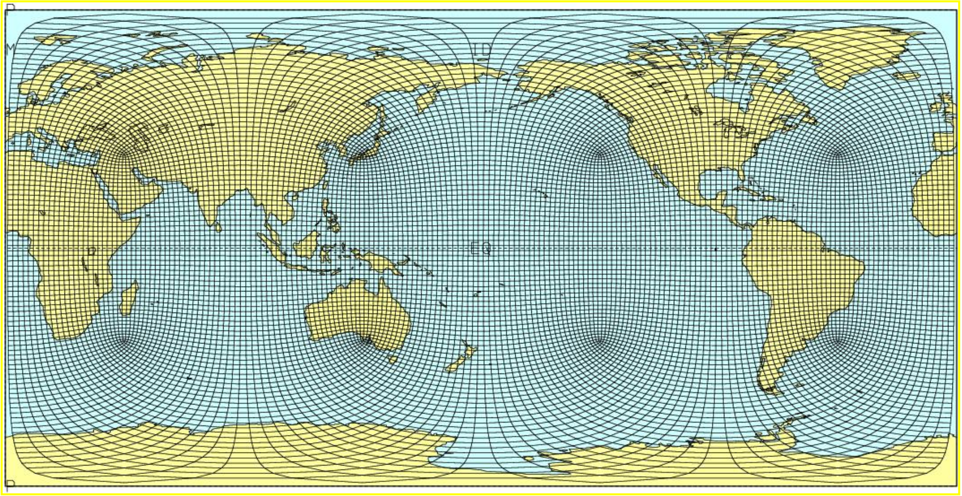

Quasi-uniform C96 CCAM grid with resolution about 100 km, showing every 2nd grid point

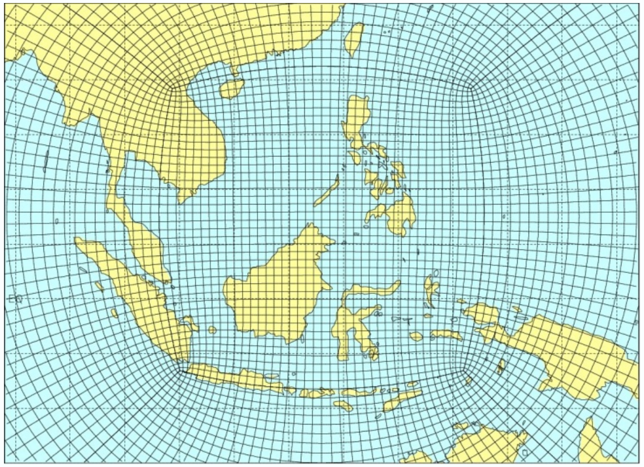

Stretched C120 grid with resolution about 25 km over SE Asia, showing every 3rd grid point

Digital-filter technique

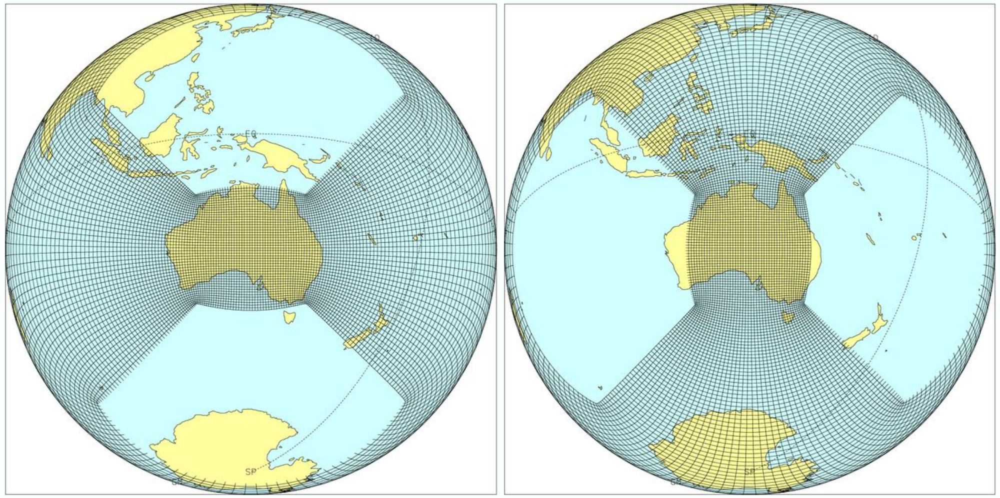

Uses a sequence of 1D passes over all panels to efficiently evaluate broad-scale digitally-filtered model fields (Thatcher and McGregor, MWR, 2009). Very similar results to 2D collocation method, or Fourier filtering.

Digital filter typically uses a length-scale the width of finest panel.

These periodically (e.g. 3-hourly or 6-hourly) can replace the corresponding broad-scale CCAM fields.

Very useful for both NWP and regional climate.

32

Reversibly-staggered ocean model

The model system includes the CSIRO reversibly staggered ocean model (Thatcher), which is coupled to the atmospheric model.

The ocean model is on the same grid as the CCAM atmosphere. Directly coupled every timestep, using same grid and same timestep.

The system allows feedbacks to/from currents in coastal regions. Preliminary results show improved simulation of cyclones.

SSTs for a 1-month coupled run

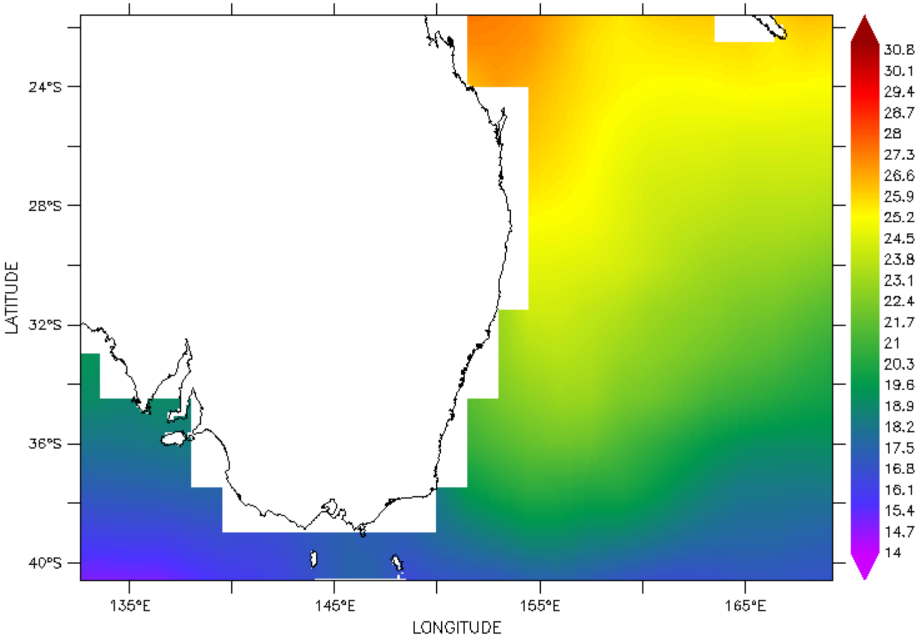

ERAI Sea surface temperature (C)

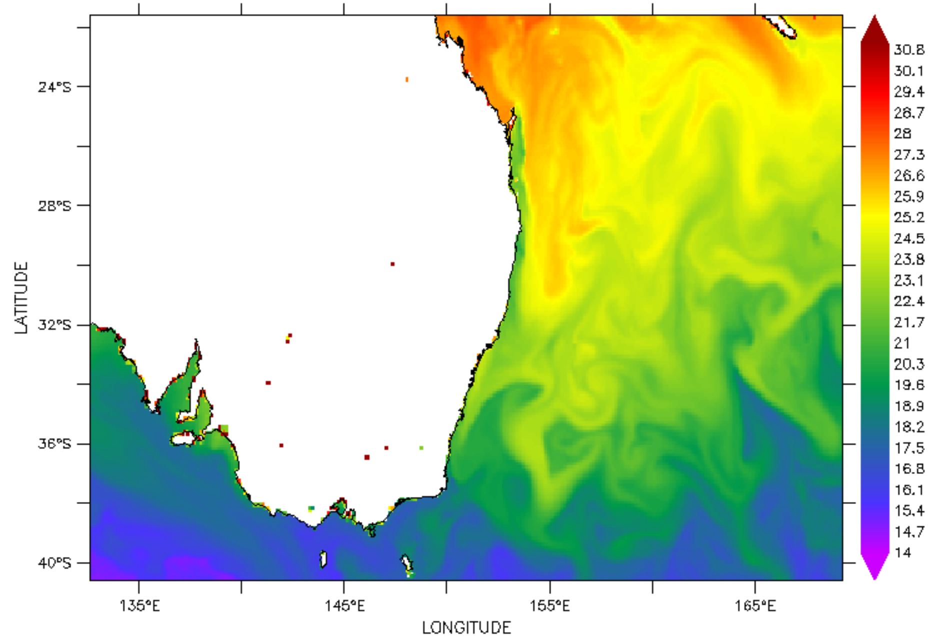

CCAM Sea surface temperature (C)

C192 run of stretched coupled CCAM having 10 km resolution over Sydney region, with 3-hourly broad-scale nudging of SSTs from ERA-Interim. Produces realistic currents.

Various CCAM collaborations

CSIR South Africa

- downscaling & preparing for CMIP6 with CCAMe

Univ. Hanoi, Vietnam

NIWA (New Zealand)

PredictWind – 1 km forecasts for sailing

BMKG (Indonesia Weather Service) and LAPAN

PAGASA (Philippines Weather Service)

Qld Climate Change Centre

Sri Lanka

Nanjing Univ. – starting

Thank you!

Split-explicit solution procedure for CCAMf

- Start τ loop

  Estimate Coriolis terms

  Stagger winds and Coriolis estimate

Nx(Δt/N) forward-backward loop

Average ps to (psu, psv) τ+n(Δt/N)

Calculate (div, sdot, omega) τ+n(Δt/N)

Calculate (ps, T) τ+(n+1)(Δt/N)

Calculate phi and staggered pressure gradient terms

Update staggered (u,v) applying Coriolis terms

End Nx(Δt/N) loop

Calculate unstaggered (u, v)

Apply Coriolis correction

Perform TVD advection (of T, qg, Cartesian_wind_components) using average ps*u, ps*v, sdot from the N substeps

Calculate physics contributions

- End τ loop

Splitting methodology
- illustrated with orthogonal flux form of equations

Denote staggered velocities by u^* and v^* (reversibly obtained from u and v).

Continuity

$$\frac{\partial p_s}{\partial t} + \underbrace{m^2 \left\{ \frac{\partial (p_s u^*/m)}{\partial x} + \frac{\partial (p_s v^*/m)}{\partial y} \right\} + p_s \frac{\partial \dot{\sigma}}{\partial \sigma}}_{A\ \Delta t'} = 0,$$

Temperature and velocity equations

$$\frac{\partial p_s T}{\partial t} + \underbrace{m^2 \left\{ \frac{\partial p_s u^* T/m}{\partial x} + \frac{\partial p_s u^* T/m}{\partial y} \right\} + p_s \frac{\partial \dot{\sigma} T}{\partial \sigma}}_{C\ adv \Delta t} - \underbrace{\frac{R_d T \omega}{c_p \sigma}}_{A\ \Delta t'} = \tilde{N}_T,$$

$$\frac{\partial p_s u}{\partial t} + \underbrace{m^2 \left\{ \frac{\partial p_s u^* u/m}{\partial x} + \frac{\partial p_s v^* u/m}{\partial y} \right\} + p_s \frac{\partial \dot{\sigma} u}{\partial \sigma}}_{C\ adv \Delta t} + \underbrace{m p_s \frac{\partial \phi_v}{\partial x} + m R_d T_v \frac{\partial p_s}{\partial x}}_{B\ \Delta t'} = f\, p_s v^T$$

with a similar equation for v.